

New Oxadiazole/ Benzimidazole Hybrids: Design, Synthesis, and Molecular Docking Studies

Fatma Hagar¹, Samar Abbas^{1*}, Ahmed Sayed², Dalia Abdelhamid¹, Mohamed Abdel-Aziz¹

¹Department of Medicinal Chemistry, Faculty of Pharmacy, Minia University, 61519-Minia, Egypt.

² Department of Pharmacognosy, Faculty of Pharmacy, Nahda University, 62513 Beni-Suef, Egypt.

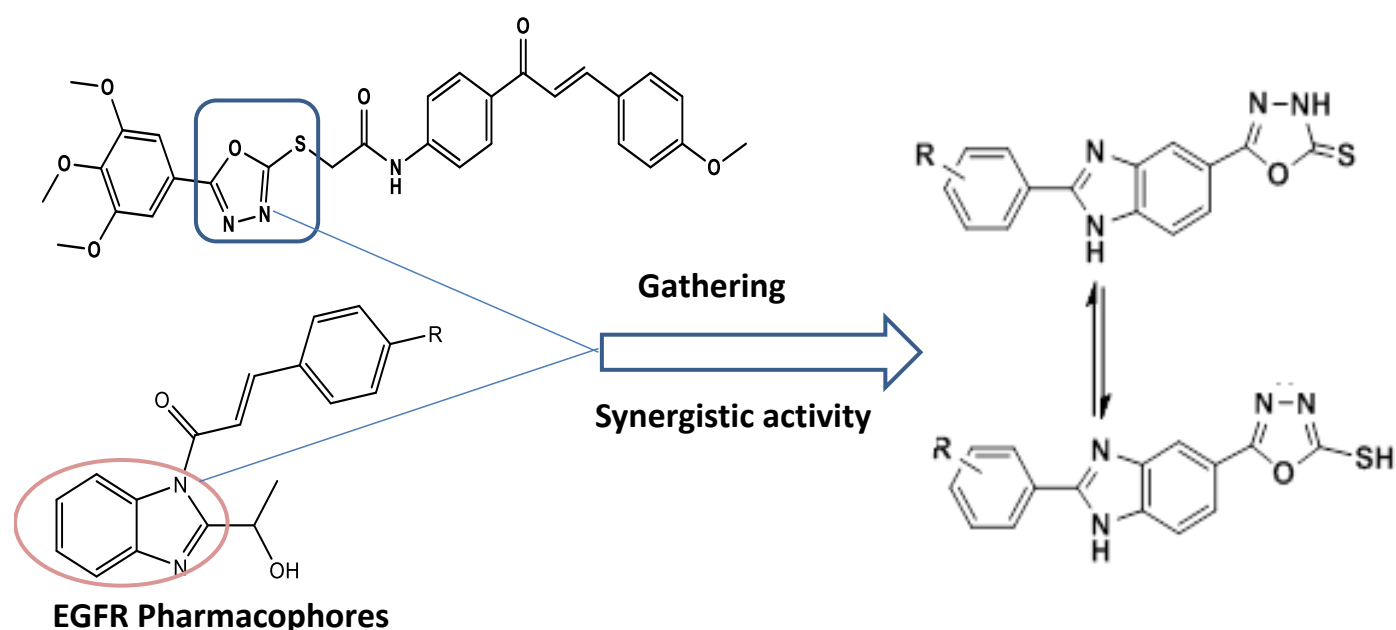
Received: January 29, 2023; revised: March 03, 2023; accepted: March 12, 2023

Abstract

Five new oxadiazole/benzimidazole hybrids were designed and synthesized as EGFR inhibitors. The structure of the new compounds was confirmed with ¹H NMR and ¹³C NMR as well as elemental analyses. Molecular docking studies were done to investigate their binding mode in ATP binding site of EGFR. The synthesized hybrids exhibited good binding in EGFR binding site. The thiol tautomers got better docking scores than thione ones. The docking scores of hybrids ranged from -7.4 kcal/mol to -8.7 kcal/mol which were comparable to that of the co-crystallized ligand Erlotinib (score = -9.7 kcal/mol). In silico physicochemical and pharmacokinetic properties prediction of them indicated that they have drug like properties.

Keywords

Heterocyclic, Benzimidazole, 1,3,4-Oxadiazole, Hybridization, EGFR inhibitors.



* Correspondence: Samar H. Abbas

Tel.: (+20) 100-542-4005 Fax: (+20) 086-236-9075

Email Address: samar_hafez@mu.edu.eg

1. Introduction

The most robust global challenges and difficulties in the 21st century is cancer because it is the leading cause of death globally, the increasing cancer cases rate than that of the population growth is the leading reason for global concern. For instance, in Egypt, the expected number of cancer patients in 2050 will exceed 350,000[1]. Additionally, the severe side effects and lack of selectivity which were associated with the currently used chemotherapeutic agents. Therefore, there is an urgent need for more selective anticancer agents with fewer side effects [2].

The epidermal growth factor receptor (EGFR) is a signaling system that promotes cell survival and proliferation.[3] Mutation in EGFR promotes the uncontrolled growth of cancer cells by enhancing cell proliferation, angiogenesis, and reducing the apoptotic pathway [4], therefore EGFR inhibitors may play a critical role in cancer treatment.

Heterocyclic compounds are considered building blocks of natural compounds such as DNA, RNA, chlorophyll and haemoglobin [5]. Additionally, heterocyclic compounds showed different biological activities such as anti-inflammatory, antifungal, antidiabetic, antibacterial, antiviral, enzyme inhibitor and anticancer activities [6]. Moreover, many heterocyclic anticancer drugs exerted their effect through inhibition of EGFR such as: **I**, Erlotinib, **II**, Gefitinib, and **III**, Lapatinib [7] (**Fig.1**).

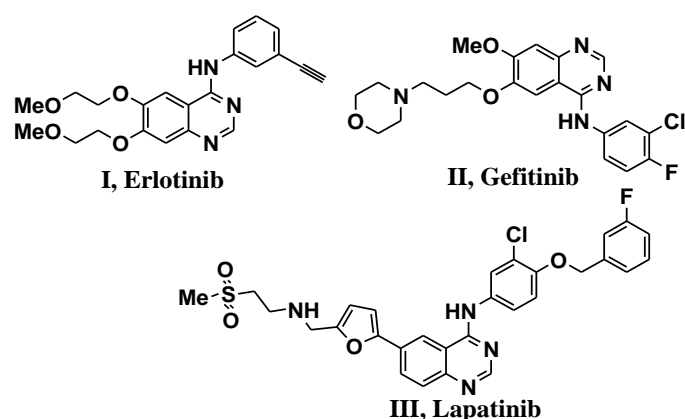


Fig. 1. Some approved anticancer drugs contain heterocyclic core.

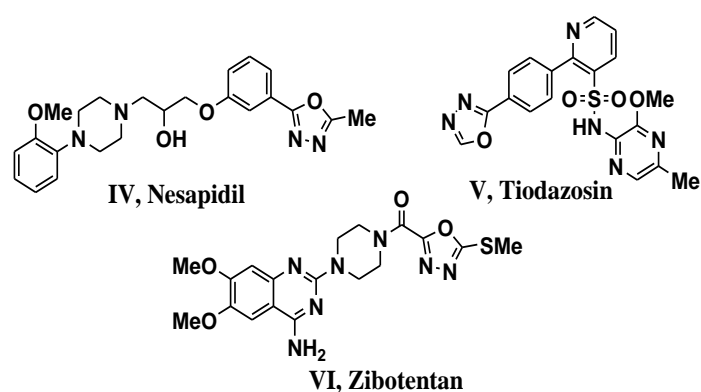


Fig. 2. Some approved anticancer drugs contain 1,3,4-oxadiazole core.

Additionally, 1,3,4-oxadiazole containing compounds displayed an important role as anticancer agents with several mechanisms of action, such as induction of apoptosis, cell cycle arrest at different phases, and inhibition of tubulin, angiogenesis, and EGFR.⁸ For example, **IV**, Nesapidil, **V**, Tiodazosin, and **VI**, Zibotentan are anticancer drugs founded in markets that contain oxadiazole ring [9] (**Fig.2**).

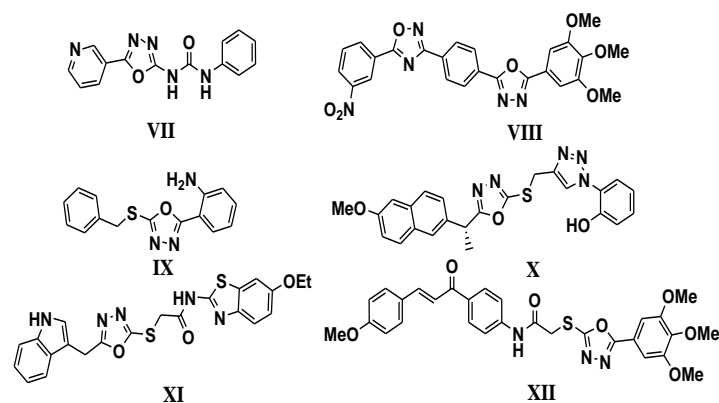


Fig. 3. Structures of 1,3,4-oxadiazoles VII-XII which displayed EGFR inhibitory activities.

Also, many oxadiazoles showed promising anticancer activity as EGFR inhibitors (**Fig. 3**). For example, compound **VII** showed potent EGFR inhibitory activity through binding of the molecule to ATP binding site. It was more potent than the reference drug Erlotinib against EGFR with IC_{50} equal to 0.28 nM and 0.42 nM, respectively. Additionally, compound **VII** showed potent anti-proliferative activity against UO-31 cell line with IC_{50} equal to 5.76 nM, while the reference drug Doxorubicin had an IC_{50} equal to 7.45 nM[10]. Furthermore, compound **VIII** showed good docking score equal to -7.03 kcal/mol against EGFR (PDB ID: 4hjo). Compound **VIII** also showed potent anticancer activity with IC_{50} ranged from 0.34 μ M to 2.45 μ M against MCF-7, A549 and MDA MB-231 cell lines while Doxorubicin as reference drug exhibited IC_{50} ranged from 2.10 μ M to 3.41 μ M[11]. Moreover, compound **IX** showed potent anticancer activity against MCF-7 and EGFR with IC_{50} equal to 1.09 μ M and 1.51 μ M, respectively while Gefitinib standard drug had IC_{50} equal to 12.05 μ M and 0.02 μ M, respectively. The binding energy of compound **IX** in EGFR binding site was equal to -10.7 kcal/mol. The inconsistency between the anti-proliferative activity of compound **IX** and its enzyme inhibition indicated that it could act as multi-kinase inhibitor, one of its targets is EGFR[12]. Also, the oxadiazole **X** displayed remarkable EGFR kinase inhibition with IC_{50} equal to 0.41 μ M while the reference drug, Erlotinib had IC_{50} = 0.30 μ M. Compound **X** showed promising anticancer activity against MCF-7 and HepG2 with IC_{50} equal to 2.13 μ g/mL and 1.63 μ g/mL, respectively compared to the activity of Doxorubicin as reference drug which had IC_{50} equal to 1.41 μ g/mL and 1.61 μ g/mL[13]. Additionally, compound **XI** showed good EGFR inhibition with IC_{50} equal to 2.80 μ M compared to Erlotinib (IC_{50} of 0.04 μ M). Furthermore, compound **XI** displayed potent anticancer activity against HCT116, A549, and A375 cancer cell lines with IC_{50} ranged from 6.43 μ M to 9.62 μ M. Its activity was more potent than Erlotinib (IC_{50} ranged from 17.86 μ M to 23.81 μ M)[14] Recently, compound **XII** displayed potent EGFR inhibition with IC_{50} equal to 0.24 μ M compared to Gefitinib standard drug (IC_{50}

= 0.023 μM). Additionally, compound **XII** showed potent anticancer activities against three leukemia cell lines K-562, KG-1a, and Jurkat cell lines with IC_{50} ranging from 1.95 to 3.45 μM comparable to Cisplatin as a positive control (IC_{50} ranging from 3.21 to 15.12 μM)[15].

Another important example of organic heterocyclic rings is benzimidazole nucleus which showed potent anticancer activities as their structure similar to natural purines[16]. They exhibited their anticancer activity by inhibition of one or more of the following targets: sirtuin (SIRT1 and SIRT2), phospholipase A2-V& COX-2 enzymes, topoisomerase I& II, tubulin polymerization, and EGFR.[17]. Additionally, many marketed drugs contain benzimidazole building block as **XIII**, Abemaciclib, **XIV**, Dovitinib, **XV**, Binimetinib, and **XVI**, Selumetinib (Fig. 4)[18].

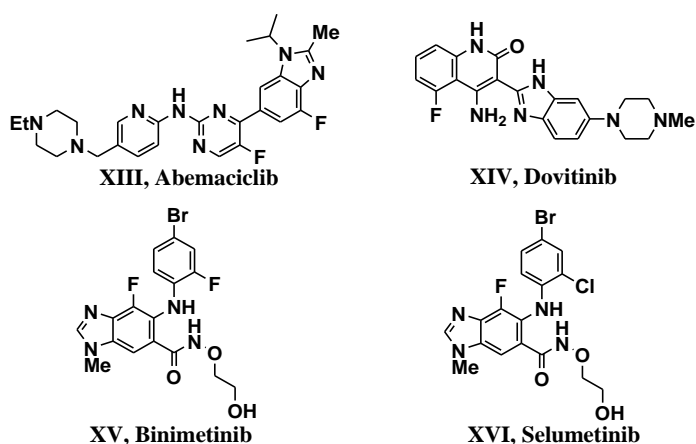
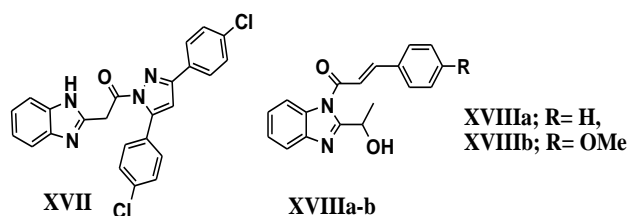


Fig. 4. Some approved anticancer drugs contain benzimidazole core

Compound **XVII** showed promising anticancer activity with IC_{50} ranging from 2.2 μM to 11.9 μM against MCF7, MDA-MB231 and A549 cell lines comparable to 5-FU as a reference drug with IC_{50} ranging from 1.16 μM to 7.12 μM . Compound **XVII** showed good EGFR inhibitory activity with IC_{50} equal to 0.97 μM which is comparable to Gefitinib (IC_{50} = 0.011 μM). Molecular docking study showed binding energy equal to -34.581 Kcal/mol with five key hydrogen bonds and two π -interaction.¹⁹ Moreover, 3-(substituted phenyl)-1-[2-(1-hydroxyethyl)]-1H-benzimidazole-1-yl) prop-2-en-1-one derivatives **XVIIIa-b** showed docking scores equal to -8.4 Kcal/mol and -8.2 Kcal/mol, respectively and showed potent affinity to EGFR receptor tyrosine kinase[20].



Several trials were done for designing and synthesis anticancer agent by gathering benzimidazole and oxadiazole in one compact unit as hybrid to overcome resistance of cancer cells[21] Also, this hybridization might afford synergetic effect and/or improvement of physiochemical and pharmacokinetic properties[22] For example, the hybrid **XIX** (Fig. 5) showed potent inhibitory activities against EGFR, erbB2 with IC_{50} equal to 0.081 μM and 0.098 μM , respectively. Moreover, compound **XIX** was more potent than the reference drug 5-FU against

MCF7 cell line with IC_{50} value equal to 5 μM . In addition to its EGFR inhibition activity, it showed induction of apoptotic activity accompanied by cell cycle arrest at G2/M phase.²³ Furthermore, compound **XX** showed remarkable anti-proliferative activities with IC_{50} values of 4.68 μM , 4.16 μM , and 5.40 μM against the HeLa, MCF-7, and A549 cell lines, respectively, comparable to Doxorubicin as positive control with IC_{50} values of 2.04 μM , 1.73 μM , and 2.34 μM . Additionally, compound **XX** was less toxic against normal human embryonic kidney cell line HEK293 (IC_{50} = 37.25 μM) than Doxorubicin (IC_{50} = 6.40 μM). A molecular docking study showed a high affinity of the compound to the EGFR kinase site (PDB_ID: 4HJO) with the value of -8.6 Kcal/mol which is comparable to that of Doxorubicin (-8.9 Kcal/mol)[24] Additionally, hybrids **XXIa-b** showed promising anticancer activity against MCF-7 cell lines with IC_{50} equal to 1.53 μM and 2.08 μM , respectively compared to Doxorubicin (IC_{50} = 1.45 μM). Moreover, the two compounds had higher binding affinity in EGFR (PDB 1M17) with binding energy equal to -8.42 kcal/mol and -8.45 kcal/mol, respectively than Erlotinib which had binding energy equal to -7.90 kcal/mol[25]. Based on the above-mentioned aspects, we designed and synthesized new hybrids by direct linking of 1,3,4-oxadiazole on benzimidazole core containing different aryl rings at position two for synergistic EGFR inhibitory activity (Fig. 6). Moreover, the new compounds were docked into the ATP binding sites of EGFR (PDB ID: 1M17) to investigate their binding affinity.

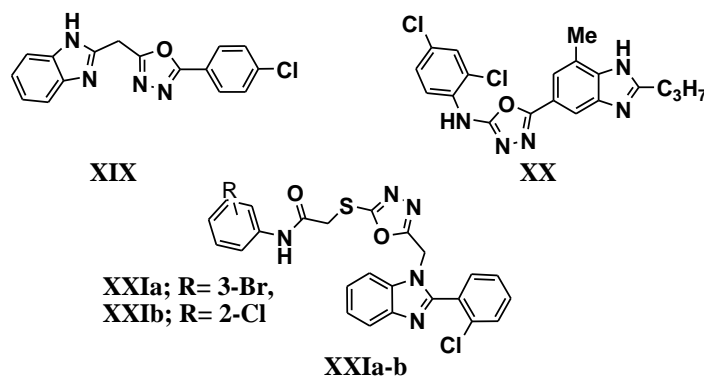


Fig. 5. Structures of 1,3,4-oxadiazole/benzimidazole hybrids XIX-XXI.

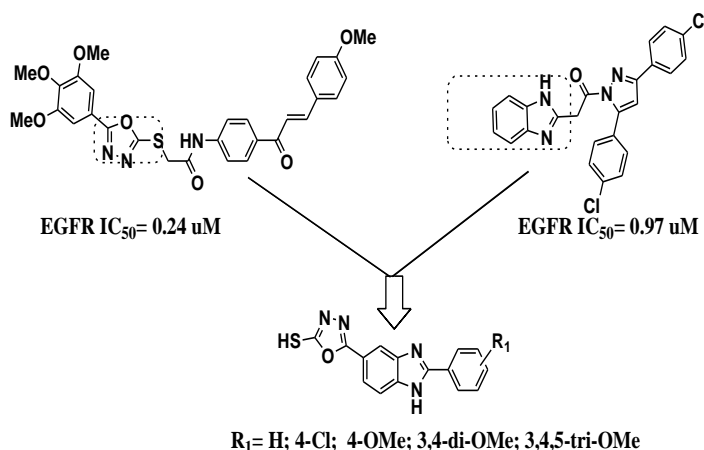
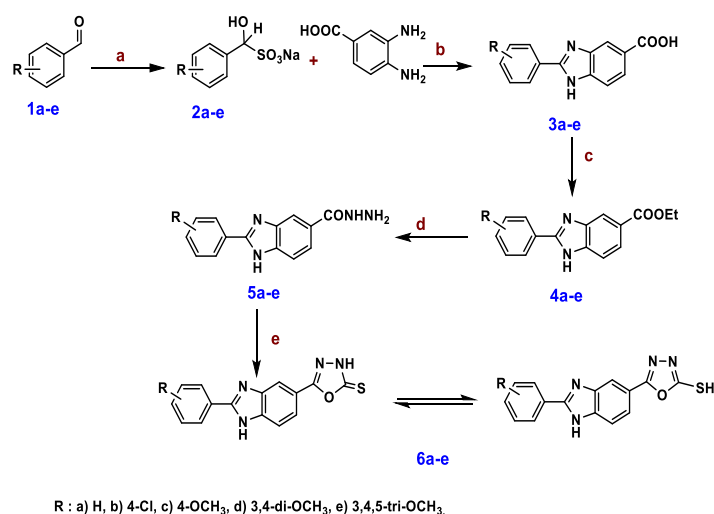


Fig. 6. Pharmacophore of the target compounds.

2. Results and Discussion

2.1. Chemistry

The sequence of the chemical reactions that were utilized in the synthesis of new oxadiazole/ benzimidazole hybrids **6a-e** is sketched in Scheme 1. The first step was the formation of the appropriate sodium hydroxy(phenyl)methanesulfonate adduct **2a-e** by the slow addition of sodium meta bisulfite to the appropriate aldehyde **1a-e** in ethanol followed by vigorous stirring for 30 min. The formed adducts then underwent condensation with 3,4-diamino benzoic acid upon reflux in DMF for 3-6 h²⁶ to afford the substituted 2-phenyl-1*H*-benzo[*d*]imidazole-5-carboxylic acids **3a-e**. The substituted ethyl 2-aryl-1*H*-benzo[*d*]imidazole-5-carboxylate **4a-e** were formed upon refluxing **3a-e** with absolute ethanol in the presence of concentrated H₂SO₄ as a dehydrating agent for 20 h.²⁷ Hydrazinolysis of ester derivatives **4a-e** underwent upon reflux with hydrazine mono hydrate for 6-7 h that afforded the carbonyl compounds **5a-e**.²⁷ Finally, our target oxadiazole/benzimidazole hybrids **6a-e** were obtained by refluxing carbonyl compounds **5a-e** with carbon disulfide and KOH in absolute ethanol overnight.¹ The solid was obtained upon evaporation of solvent under vacuum. The resulting solid was dissolved in water and acidified with 10% HCl. The formed precipitate was filtered off, washed with water, dried, and recrystallized from ethanol to generate the corresponding oxadiazole/benzimidazole derivatives **6a-e** in good yield ranged from 60% to 87%. ¹H NMR and ¹³C NMR spectroscopy as well as elemental analysis were used for confirming the structure of the new compounds. ¹H NMR spectra of compounds **6a-c** showed singlet signals at δ: 7.22-8.22 ppm related to H atom at position 4 of benzimidazole ring, in addition all aromatic or aliphatic hydrogen's appeared in the expected chemical shift. The ¹³C NMR spectra of compounds **6a-e** revealed the presence of the carbon of thione group in all compounds at δ: 162.57-168.83 ppm. All other carbons appeared in their expected chemical shift.



Reagent and reaction conditions: (a) EtOH, Sodium meta bisulfite in water, vigorous stirring 0.5 h; (b) DMF, reflux 3-6 h; (c) EtOH, Conc. H₂SO₄, reflux 20 h; (d) NH₂NH₂, EtOH, reflux 3-7 h; (e) 1- CS₂, KOH, EtOH, reflux 12 h.; 2- Conc HCl, (60.0-87.0%).

Scheme 1. Synthesis of oxadiazole/benzimidazole hybrids **6a-e**.

2.2. Docking results

The structures of the synthesized derivatives (i.e., **6a-e**) were prepared and docked inside the active site of EGFR (PDB ID: 1M17) to investigate their binding interactions (**Fig. 7A-E**). We took into consideration the effect of thiol-thione tautomerism of these derivatives during the docking step, where each tautomer was docked separately. The resulting docking scores of these derivatives, including their tautomers, were to some extent convergent (i.e., docking scores ranged from -7.4 to -8.7 kcal/mol, **Table 1**) and comparable with that of the co-crystallized ligand Erlotinib (score = -9.7 kcal/mol).

Table 1. Docking scores of compounds (**6a-e**) inside the active site of EGFR

Compound	Docking score (kcal/mol)	
	Thiol tautomer	Thione tautomer
6a	-8.2	-8.7
6b	-8.1	-8.3
6c	-7.8	-8.0
6d	-7.7	-8.0
6e	-7.4	-7.6
Erlotinib	-9.7	

In general, thiol tautomers got better scores than thione ones. Additionally, the substitution on the phenyl ring led to lower docking scores, where the trimethoxy substitution in compound **6e** was associated with lowest scores (-7.4 kcal/mol and -7.6 kcal/mol for thiol and thione tautomer, respectively). The binding modes of all derivatives (i.e., **6a-e**) were comparable, where hydrophobic interactions with LEU 694, VAL 702, LYS 721, and LEU 820 were the key interacting residues (**Fig. 7A-E**). Both **6a** and **6d** showed similar binding poses, while the remaining structures (**6b**, **6c**, and **6e**) showed also similar but flipped poses (**Fig. 7A-E**). In regard to hydrophilic interactions (i.e., H-bonding), LYS 721, THR 766, MET 769, and THR 830 were the common interacting residues. Judging from the previous in silico structural analysis, it can be concluded that the derivatives **6a-e** are considered promising structure motifs acting as EGFR inhibitors.

2.3. In silico prediction of physicochemical and pharmacokinetic properties

In this investigation, we used Swiss ADME to estimate the physicochemical and pharmacokinetic features of target substances (<http://www.swissadme.ch/index.php>). Briefly, the five independent models SILICOS-IT, MLOGP, iLOGP, XLOGP3, and WLOGP all predict lipophilicity. Consensus log Po/w is determined using their arithmetic mean[28]. A map of polarity expressed in TPSA vs lipophilicity expressed in WLOGP, another model for predicting lipophilicity, is called BOILED Egg. In the BOILED Egg plot (**Fig. 8**), the yolk indicates the potential for BBB permeability while the white represents the potential for GI absorption. Lastly, a plot of bioavailability radar is a plot of six different physicochemical properties size, polarity, flexibility, solubility, saturation and lipophilicity[29,30] The ideal range for good oral bioavailability is represented by the pink hexagon in the center of the image.

These calculations revealed that target compounds outperformed erlotinib in terms of the metrics, which are shown in **Table 2** and **Fig.9**. Additionally, they were projected to have higher GI absorption than erlotinib due to the target compounds' notable reduction in lipophilicity (WLOGP 3.57-4.22) as compared to Erlotinib (WLOGP 3.48). Additionally, the polarity of these target compounds was acceptable (TPSA 106.40-124.86) except **6e** with unacceptable TPSA 134.09 and erlotinib with TPSA equal to 74.73.

The target molecular compounds' weights of less than 500 g/mol. Otherwise, no target compounds deviated from the Lipinski rule. All of the target compounds had less Fraction Csp3 than erlotinib. The molecular flexibility of most target drugs had lower RB than erlotinib, which also increases the oral activity of the target compounds. The five compounds have 2-5 RB, while erlotinib has 10 RB, the ideal range < 9 RB.

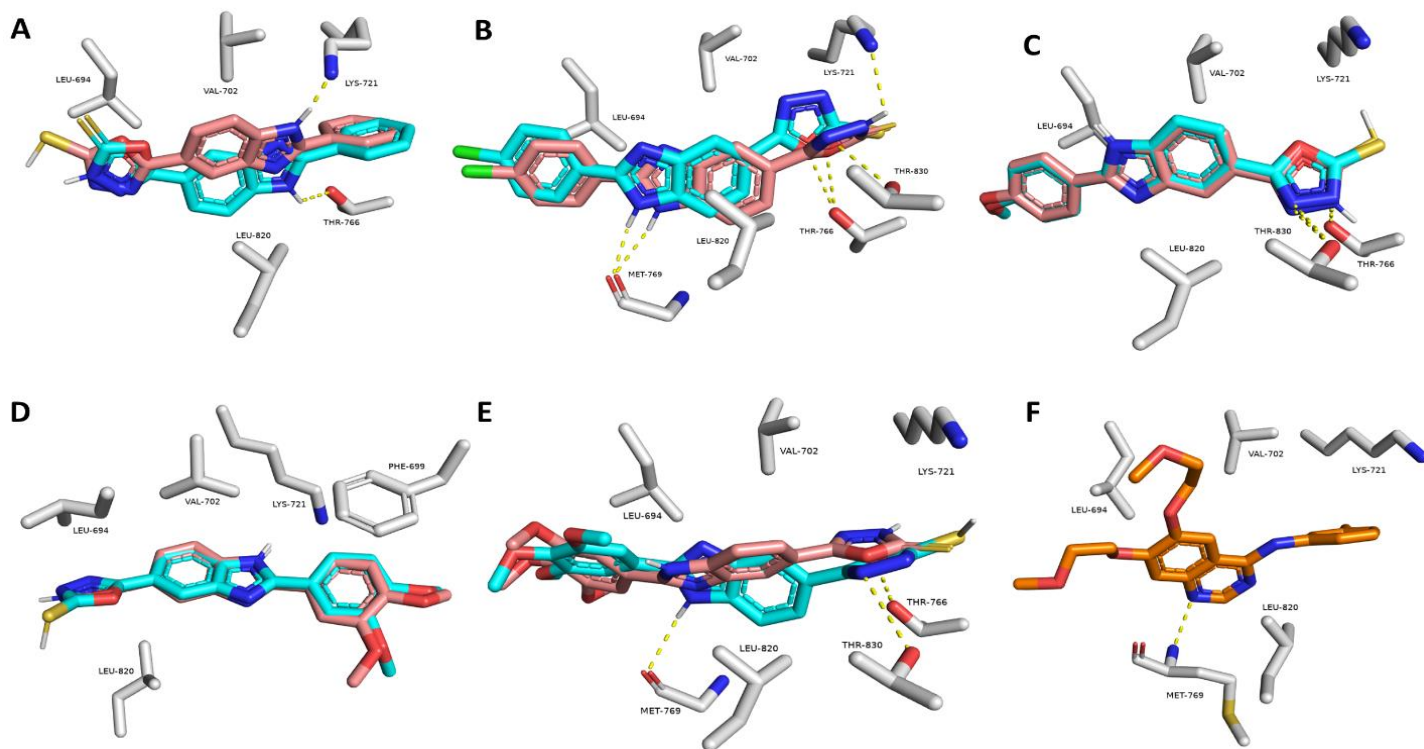


Fig. 7. A-E: Binding modes of compounds **6a-e**, respectively (Brick red colored structures are thione tautomers, while cyan-colored structures are thiol tautomers) inside the binding site of the kinase domain of human EGFR (PDB ID: 1M17) together with the co-crystallized ligand (**F**; orange-colored structure).

Table 2. Predicted pharmacokinetics and physicochemical properties of target compounds 6a-e and Erlotinib

	Erlotinib	6a	6b	6c	6d	6e
M.Wt	393.44	294.33	328.78	324.36	354.38	384.41
Fraction Csp3	0.27	0.00	0.00	0.06	0.12	0.17
RB	10	2	2	3	4	5
HBA	6	4	4	5	6	7
HBD	1	1	1	1	1	1
MR	111.40	82.07	87.08	88.57	95.06	101.55
TPSA	74.73	106.40	106.40	115.63	124.86	134.09
Log P	3.23	3.02	3.57	3.07	2.99	2.99
GI absorption	High	High	High	High	High	High
BBB	Yes	No	No	No	No	No
Lip V	0	0	0	0	0	0
Bio.SC	0.55	0.55	0.55	0.55	0.55	0.55

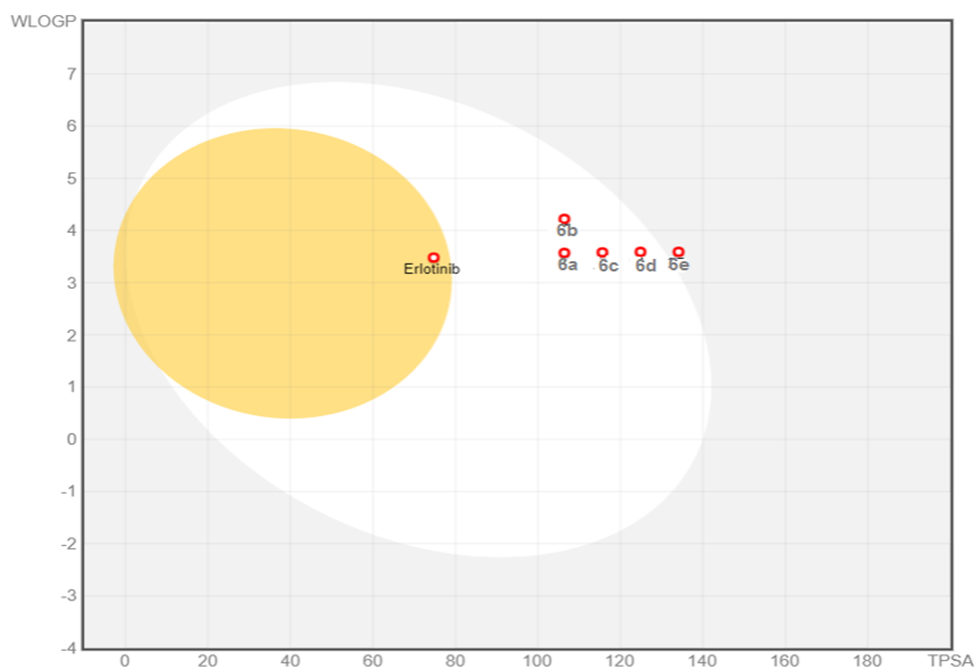


Fig.8. Forecast Boiled-Egg plotting from Swiss ADME online website for scaffolds **6a-e** and **Erlotinib**

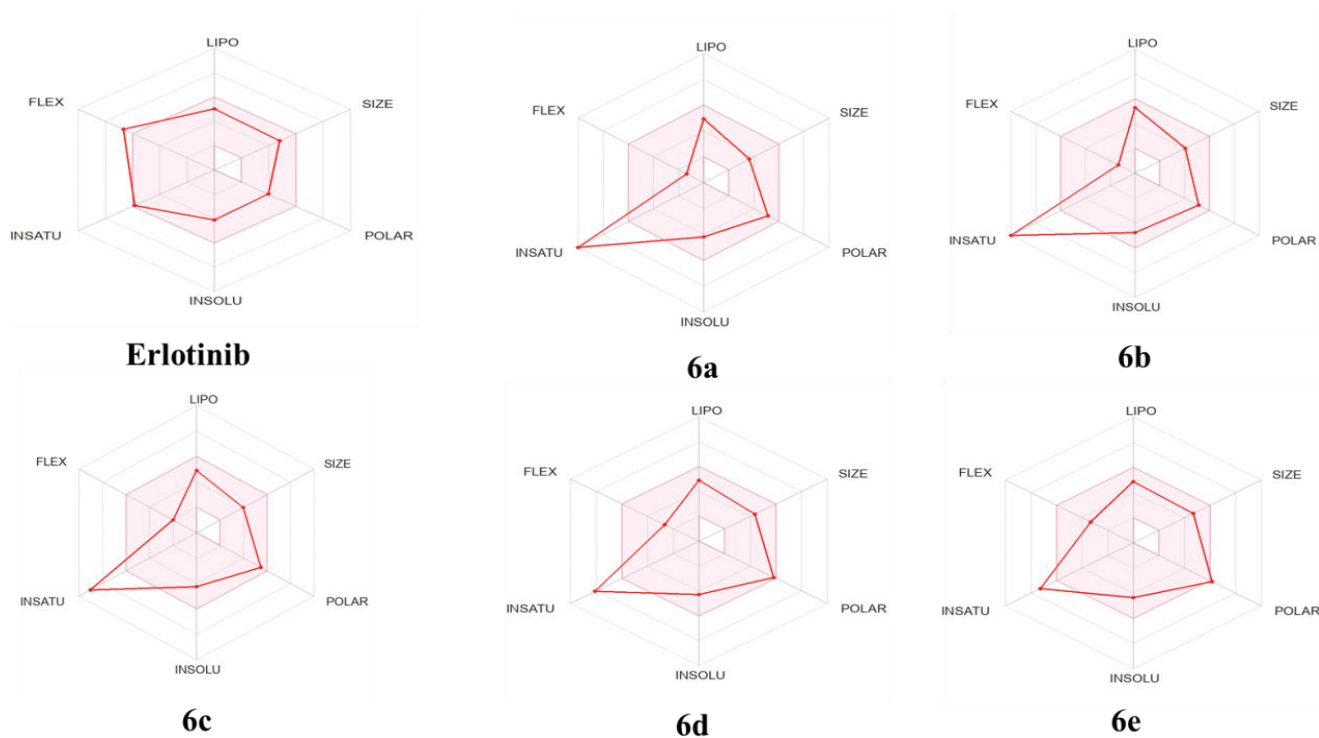


Fig.9. Radar bioavailability diagram from Swiss ADME website for scaffolds **6a-e** and **Erlotinib**. The pink area characterizes the optimum property values range for the oral bioavailability, and the red lines represent the forecasted characters.

3. Conclusion

New five oxadiazole/benzimidazole hybrids were synthesized and their structures were confirmed with ^1H NMR and ^{13}C NMR as well as elemental analyses. Molecular docking study of the new hybrids inside the active site of EGFR (PDB ID: 1M17) revealed that the new hybrids had docking scores ranged from -7.4 to -8.7 kcal/mol which were comparable to that of the co-crystallized ligand Erlotinib (score = -9.7 kcal/mol). Additionally, all derivatives **6a-e** had comparable binding modes and could be considered promising structure motifs acting as EGFR inhibitors. Furthermore, Swiss ADME estimation of the physicochemical and pharmacokinetic features of hybrids **6a-e** indicated that compounds **6a-e** had drug like properties. Thus the hybrids **6a-e** might be potent anticancer agents *via* EGFR inhibition. However, further *in vitro* and *in vivo* anti-proliferation experiment studies are needed to proof and clarify their efficacy as anticancer agents.

4. Experimental Section

4.1. Chemistry section:

- All used solvent and chemicals were of Analytical grade. chemicals and solvents were used.
- Thin layer chromatography precoated Merck silica gel 60 F254 aluminum sheets were used for monitoring the progress of reactions.
- Stuart electro-thermal melting point apparatus was used for detection of melting points and they were uncorrected.
- ^1H NMR spectra were recorded on Burker AG, Switzerland, 500 MHz, Faculty of Pharmaceutical Sciences, Umm Al-Qura University, Mecca, Saudi Arabia; chemical shift (δ) was expressed in ppm relative to TMS ($\delta = 0$ PPM) as internal standard and DMSO- d_6 as a solvent. Chemical shifts (δ) were expressed in parts per million (ppm) and coupling constants (J) were expressed in Hertz. The signals were designated as follows: s, singlet; d, doublet; t, triplet; q, quartet, m, multiplet.
- ^{13}C NMR spectra were recorded on Burker AG, Switzerland and 125 MHz, faculty of Pharmaceutical Sciences, Umm Al-Qura University, Mecca, Saudi Arabia using TMS as the reference standard and DMSO- d_6 as a solvent. Chemical shifts (δ) were expressed in parts per million (ppm).
- Elemental analyses were recorded on Shimadzu GC/MS-QP5050A at the Regional center for Mycology and Biotechnology, Al-Azhar University, Egypt

4.1.1. General procedure for the synthesis of the adduct 2a-e [31]

A Solution of sodium meta bisulfite (1.6 gm/10mL water) was added drop wisely to the appropriate benzaldehyde derivative solution in ethanol with vigorous stirring for 30 min. The precipitate that formed was filtered off and dried *in vacuo* and used in the next step without purification.

4.1.2. General procedure for the synthesis of substituted phenyl-1H-benzo[d]imidazole-5-carboxylic acid 3a-e [32]

A mixture of the appropriate adduct 2a-e (2 mmol) and 3,4-diamino benzoic acid (2 mmol) in DMF (5 mL) was heated under reflux for (3-6) h after which the reaction mixture was cooled, poured into ice water. The formed solid was collected

and recrystallized from the appropriate solvent to afford the corresponding acid in good yield.

4.1.2.1. 2-Phenyl-1H-benzo[d]imidazole-5-carboxylic acid (3a).

White powder (83.0% yield); mp: >300 °C (Reported mp: 325 °C) [33].

4.1.2.2. 2-(4-Chlorophenyl)-1H-benzo[d]imidazole-5-carboxylic acid (3b).

White powder (80.0% yield); mp: 180-181 °C (Reported mp: 168-169 °C) [34].

4.1.2.3. 2-(4-Methoxyphenyl)-1H-benzo[d]imidazole-5-carboxylic acid (3c).

White powder (78.0% yield); mp: 244-246 °C (Reported mp: 246-247 °C) [35].

4.1.2.4. 2-(3,4-Dimethoxyphenyl)-1H-benzo[d]imidazole-5-carboxylic acid (3d).

White powder (69.0% yield); mp: 215-217 °C (Reported mp: 200(bubl)°C) [36].

4.1.2.5. 2-(3,4,5-Trimethoxyphenyl)-1H-benzo[d]imidazole-5-carboxylic acid (3e).

White powder (66.0% yield); mp: 275-277 °C (Reported mp: 280-281°C) [37].

4.1.3 General procedure for the synthesis of substituted ethyl 2-phenyl-1H-benzo[d]imidazole-5-carboxylate (4a-e).²⁷

A mixture of the appropriate substituted phenyl-1H-benzo[d]imidazole-5-carboxylic acid (0.01 mol) and 2 mL of concentrated H_2SO_4 in 100 mL of absolute ethanol was heated under reflux for 20 h. The reaction mixture was concentrated under vacuum, then washed with saturated NaHCO_3 (2 X 20 mL). The resulting solid was filtered off, dried to give the ethyl ester derivatives **2a-e**, and used for following step without further purification.

4.1.3.1. Ethyl-2-phenyl-1H-benzo[d]imidazole-5-carboxylate [38] (4a).

White powder (71.0% yield); mp: 183-184 °C.

4.1.3.2. Ethyl-2-(4-chlorophenyl)-1H-benzo[d]imidazole-5-carboxylate (4b).

White powder (78.0% yield); mp: >300 °C.

4.1.3.3. Ethyl-2-(4-methoxyphenyl)-1H-benzo[d]imidazole-5-carboxylate (4c).

White powder (68.0% yield); mp: 202-205 °C (Reported mp: 188-189 °C) [39].

4.1.3.4. Ethyl-2-(3,4-dimethoxyphenyl)-1H-benzo[d]imidazole-5-carboxylate³¹ (4d).

White powder (69.0% yield); mp: 230-232 °C.

4.1.3.5. Ethyl-2-(3,4,5-trimethoxyphenyl)-1H-benzo[d]imidazole-5-carboxylate (4e).

White powder (74.0% yield); mp: 260 °C.

4.1.4. General procedure for the synthesis of substituted 5-hydrazineyl-2-phenyl-1H-benzo[d]imidazole(5a-e) [40]

A mixture of the appropriate substituted ethyl 4-(1H-benzo[d]imidazol-2-yl)benzoate **4a-c** (0.1 mol) hydrazine monohydrate 99% (0.25 mol), was heated under reflux for 6 h. Hydrazine monohydrate was removed under vacuum and the residue was poured into 200 mL of cold water. The formed solid was collected, washed with ice-cold water and recrystallized from 95% ethanol.

4.1.4.1. 2-{Phenyl-1H-benzo[d]imidazole}-5-carbohydrazide (5a).

Beige Crystal (1.8g, 73% yield); m.p: 247-249 °C; ¹H NMR (500 MHz, DMSO-*d*₆) δ (ppm): 3.74 (2H, s, NH₂), 7.21-7.26 (1H, m, Ar-H), 7.58-7.69 (1H, m, Ar-H), 7.99 (3H, d, *J* = 8.2 Hz, Ar-H), 8.09 (2H, d, *J* = 8.2 Hz, Ar-H), 8.21-8.27 (1H, s, Ar-H), 9.76 (1H, s, NH); ¹³C NMR (125 MHz, DMSO-*d*₆) δ (ppm): 108.43, 117.83, 126.15, 126.72, 127.94, 129.67, 135.55, 136.29, 142.73, 142.93, 152.79, 168.79.

4.1.4.2. 2-{[4-Chlorophenyl]-1H-benzo[d]imidazole}-5-carbohydrazide (5b).

Beige Crystal (2.0g, 70% yield); m.p: 250-252 °C; ¹H NMR (500 MHz, DMSO-*d*₆) δ (ppm): 3.85 (2H, s, NH₂), 7.13 (2H, d, *J* = 8.7 Hz, Ar-H), 7.50-7.65 (1H, m, Ar-H), 7.70 (1H, d, *J* = 8.1 Hz, Ar-H), 7.99-8.07 (1H, m, Ar-H), 8.14 (2H, d, *J* = 8.7 Hz, Ar-H), 9.76 (1H, s, NH); ¹³C NMR (125 MHz, DMSO-*d*₆) δ (ppm): 108.01, 111.10, 114.90, 115.08, 122.74, 127.40, 128.72, 134.99, 135.70, 153.80, 161.35, 167.08.

4.1.4.3. 2-{[4-Methoxyphenyl]-1H-benzo[d]imidazole}-5-carbohydrazide⁴⁰ (5c).

White powder (80.0% yield); mp: 257-259 °C (Reported mp: 250-252 °C).

4.1.4.4. 2-{[3,4-Dimethoxyphenyl]-1H-benzo[d]imidazole}-5-carbohydrazide (5d).

Gray Crystal (2.2g, 72% yield); m.p: 230-231 °C; ¹H NMR (500 MHz, DMSO-*d*₆) δ (ppm): 3.85 (3H, s, OCH₃), 3.89 (3H, s, OCH₃), 7.13-7.16 (1H, m, Ar-H), 7.51-7.61 (1H, m, Ar-H), 7.68-7.72 (1H, m, Ar-H), 7.75-7.81 (2H, m, Ar-H), 8.03-8.13 (1H, m, Ar-H), 9.72 (1H, s, NH); ¹³C NMR (125 MHz, DMSO-*d*₆) δ (ppm): 56.07, 56.09, 110.30, 112.28, 114.13, 116.11, 120.07, 121.68, 122.81, 123.08, 127.51, 148.34, 149.38, 151.02, 153.71, 167.09.

4.1.4.5. 2-{[3,4,5-Trimethoxyphenyl]-1H-benzo[d]imidazole}-5-carbohydrazide (5e).

Brown Crystal (2.3g, 68% yield); m.p: 264-266 °C; ¹H NMR (500 MHz, DMSO-*d*₆) δ (ppm): 3.89 (6H, s, 2OCH₃), 3.92 (3H, s, OCH₃), 7.32-7.37 (1H, m, Ar-H), 7.51-7.56 (3H, m, Ar-H), 7.70-7.74 (1H, m, Ar-H), 9.79 (1H, s, NH); ¹³C NMR (125 MHz, DMSO-*d*₆) δ (ppm): 56.54, 60.71, 104.47, 104.69, 120.19, 125.53, 127.40, 138.27, 139.63, 146.15, 148.64, 151.35, 153.72, 167.11.

4.1.5. General procedure for the synthesis of substitute 5-(2-phenyl-1H-benzo[d]imidazol-5-yl)-1,3,4-oxadiazole-2-thiol(6a-e) [1]

Equimolar quantities of 5-substituted ethyl 4-(1H-benzo[d]imidazol-2-yl)benzohydrazides **5a-e** (0.05mol) and KOH (0.05mol) refluxed with carbon disulfide (0.17 mol, 10mL) in ethanol 70mL overnight until evaluation of H₂S gas stopped. The reaction mixture was concentrated under vacuum. The formed solid was collected and dissolved in H₂O then acidified with 10% HCl to pH 2. The formed solid was collected and washed with water and recrystallized with an appropriate solvent to afford the target oxadiazoles **6a-e** in good yield.

4.1.5. 1. 5-{2-Phenyl-1H-benzo[d]imidazol-5-yl}-1,3,4-oxadiazole--2(3H)-thione (6a).

Beige Crystal (1g, 81% yield); m.p: 270-272 °C; ¹H NMR (500 MHz, DMSO-*d*₆) δ (ppm): 7.55-7.62 (3H, m, Ar-H), 7.71-7.77 (2H, m, Ar-H), 7.95 (1H, s, Ar-H), 8.00 (2H, d, *J* = 8.1 Hz, Ar-H), ¹³C NMR (125 MHz, DMSO-*d*₆) δ (ppm): 112.61, 115.84, 118.51, 122.61, 125.07, 127.72, 129.60, 132.80, 135.57, 137.30, 152.52, 161.05, 163.83; Anal. calcd. for C₁₅H₁₀N₄OS: C 61.21, H 3.42, N 19.04, S 10.89. Found: C 61.42, H 3.52, N 19.20, S 10.99.

4.1.5. 2. 5-{2-[4-Chlorophenyl]-1H-benzo[d]imidazol-5-yl}-1,3,4-oxadiazole-2(3H)-thione (6b).

Beige Crystal (1.2g, 76% yield); m.p: 253-255 °C; ¹H NMR (500 MHz, DMSO-*d*₆) δ (ppm): 7.60 (1H, d, *J* = 8.3 Hz, Ar-H), 7.64 (1H, d, *J* = 8.3 Hz, Ar-H), 7.71-7.75 (1H, m, Ar-H), 7.90-7.92 (1H, m, Ar-H), 8.01-8.08 (1H, m, Ar-H), 8.09 (1H, d, *J* = 8.3 Hz, Ar-H), 8.22 (1H, s, Ar-H); ¹³C NMR (125 MHz, DMSO-*d*₆) δ (ppm): 113.57, 115.07, 117.31, 129.26, 129.60, 130.57, 136.82, 137.31, 140.57, 151.82, 152.57, 161.52, 168.05; Anal. calcd. for C₁₅H₉ClN₄OS: C 54.80, H 2.76, N 17.04, S 9.75. Found: C 55.03, H 2.96, N 17.24, S 9.65.

4.1.5.3. 5-{2-[4-Methoxyphenyl]-1H-benzo[d]imidazol-5-yl}-1,3,4-oxadiazole-2(3H)-thione (6c).

Beige Crystal (1.7g, 80% yield); m.p: 284-286°C; ¹H NMR (500 MHz, DMSO-*d*₆) δ (ppm): 3.81(3H, s, OCH₃), 7.10 (1H, d, *J* = 8.9 Hz, Ar-H), 7.13 (1H, d, *J* = 8.9 Hz, Ar-H), 7.72 (1H, s, Ar-H), 7.88-7.90 (1H, m, Ar-H), 7.97-8.07 (3H, m, Ar-H), ¹³C NMR (125 MHz, DMSO-*d*₆) δ (ppm): 55.61, 112.82, 114.82, 115.86, 116.08, 117.11, 121.06, 129.05, 129.31, 137.58, 140.53, 153.82, 161.53, 162.57; Anal. calcd. for C₁₆H₁₂N₄O₂S: C 59.25, H 3.73, N 17.27, S 9.88. Found: C 59.35, H 3.63, N 17.17, S 9.93.

4.1.5.4. 5-{2-[3,4-Dimethoxyphenyl]-1H-benzo[d]imidazol-5-yl}-1,3,4-oxadiazole-2(3H)-thione (6d).

Beige Crystal (1.7g, 80% yield); m.p: 283-285°C; ¹H NMR (500 MHz, DMSO-*d*₆) δ (ppm): 3.86(3H, s, OCH₃), 3.90 (3H, s, OCH₃) 7.14-7.18 (1H, m, Ar-H), 7.61-7.68 (2H, m, Ar-H), 7.72-7.74 (1H, m, Ar-H), 8.02 (1H, d, *J* = 9.0 Hz, Ar-H), 8.15 (1H, d, *J* = 9.0 Hz, Ar-H); ¹³C NMR (125 MHz, DMSO-*d*₆) δ (ppm): 56.15, 56.24, 110.45, 112.36, 116.24, 116.38, 120.28, 120.39, 122.28, 122.45, 123.87, 124.63, 148.15, 149.46, 151.37, 161.99, 168.35; Anal. calcd. for C₁₇H₁₄N₄O₃S: C 57.62, H 3.98, N 15.81, S 9.05. Found: C 57.52, H 3.88, N 15.99, S 9.15.

4.1.5.5. 5-{2-[3,4,5-Trimethoxyphenyl]-1H-benzo[d]imidazol-5-yl}-1,3,4-oxadiazole-2(3H)-thione (6e).

Brown Crystal (1.5g, 70% yield); m.p: 232-234°C; ¹H NMR (500 MHz, DMSO-*d*₆) δ (ppm): 3.73 (3H, s, OCH₃), 3.88 (6H, s, 2OCH₃), 7.25 (2H, s, Ar-H), 7.67-7.72 (1H, m, Ar-H), 7.89-7.96 (1H, m, Ar-H), 8.18- 8.33(1H, m, Ar-H), 13.40 (1H, s, NH); ¹³C NMR (125 MHz, DMSO-*d*₆) δ (ppm): 56.60, 60.61, 106.87, 107.13, 117.78, 121.55, 130.83, 139.20, 144.31, 144.67, 149.57, 151.99, 153.56, 153.72, 166.65; Anal. calcd. for C₁₈H₁₆N₄O₄S: C 56.24, H 4.20, N 14.58, S 8.34. Found: C 56.29, H 4.15, N 14.68, S 8.39.

4.2. Docking based virtual screening

4.2.1. Ligand Structure Generation

OpenBabel v.3.1.1 was used to convert the structures' SMILE codes to three-dimensional configurations that were subsequently subjected to a minimization of energy using the steepest descent technique with the same software. The minimization was performed by the force field MMFF94. Using AutoDockTools v.4.2, all torsions of the selected structures were assigned and their Gasteiger charges were provided for all studied atoms in structures.^{41,42}

4.2.2. Protein Structure Preparation

For docking screening, the human EGFR crystal structure (PDB code: 1M17) were used. PDBfixer was used to edit the downloaded structure, adding missing residues and atoms, and removing co-crystallized H₂O and heteroatoms. Through AutoDock Tools v.4.2, polar hydrogen and Gasteiger charges were subsequently made available for both proteins.⁴³

4.2.3. Structural Docking

The docking process was carried out using the PyRx platform's built-in AutoDock Vina software According to the co-crystallized ligands of both enzymes, the docking search grid boxes were determined to perfectly enclose them with a 20 Å³ total size.^{44,45}

The grid box coordinates were set to be x = -10.857; y = 22.836; z = -16.347. Pymol software was used to evaluate and display docking poses. Exhaustiveness was set to 24. Ten poses were generated for each docking experiment. Docking poses were analyzed and visualized using Pymol software. The docking protocol was validated by re-docking the co-crystallized ligand (i.e. Erlotinib) into the active sites of the enzyme (i.e. EGFR). The resulting top-scoring poses of both ligands were in good

alignment with the co-crystallized one with slight deviation (RMSDs = 1.143Å) [46].

Conflicts of Interest

The authors declare no conflicts of interest

References:

- [1]Hagar, F. F.; Abbas, S. H.; Abdelhamid, D.; Gomaa, H. A. M.; Youssif, B. G. M.; Abdel-Aziz, M. New 1,3,4-oxadiazole-chalcone/benzimidazole hybrids as potent antiproliferative agents. *Arch. Pharm.* **2023**, *356* (2), e2200357. <https://doi.org/10.1002/ardp.202200357>.
- [2]Mohammed, H.H.H.; Abd El-Hafeez, A.A.; Abbas, S. H.; Abdelhafez, E.-S.M.N.; Abuo-Rahma, G.E.-D.A. New antiproliferative 7-(4-(N-substituted carbamoylmethyl)piperazin-1-yl) derivatives of ciprofloxacin induce cell cycle arrest at G2/M phase, *Bioorg. Med. Chem.* **2016**, *24*, 4636–4646. <https://doi.org/10.1016/j.bioorg.2020.104422>.
- [3]Luwor, R. B.; Zhu, H.-J.; Walker, F.; Vitali, A. A.; Perera, R. M.; Burgess, A. W.; Scott, A. M.; Johns, T. G. The Tumor-Specific De2–7 Epidermal Growth Factor Receptor (EGFR) Promotes Cells Survival and Heterodimerizes with the Wild-Type EGFR. *Oncogene* **2004**, *23* (36), 6095–6104. <https://doi.org/10.1038/sj.onc.1207870>.
- [4]Baylin, S. B.; Jones, P. A. A Decade of Exploring the Cancer Epigenome—Biological and Translational Implications. *Nat. Rev. Cancer* **2011**, *11* (10), 726–734. <https://doi.org/10.1038/nrc3130>.
- [5]Muttannavar, V.; Melavanki, R. M.; Bhavya, P.; Kusanur, R.; Patil, N. R.; Naik, L. R. Non-Linear Optical Properties Study of Two Heterocyclic Compounds. *Int J Life Sci Pharma Res* **2018**, *8* (3), 24–30. <https://doi.org/10.22376/ijpbs/lpr.2018.8.3.L24-30>
- [6]Al-Mulla, A. A Review: Biological Importance of Heterocyclic Compounds. *Pharma Chem.* **2017**, *9* (13), 141–147.
- [7]Rocha-Lima, C. M.; Soares, H. P.; Raez, L. E.; Singal, R. EGFR Targeting of Solid Tumors. *Cancer Control* **2007**, *14* (3), 295–304. <https://doi.org/10.1177/107327480701400313>
- [8]Vaidya, A.; Pathak, D.; Shah, K. 1, 3, 4-oxadiazole and Its Derivatives: A Review on Recent Progress in Anticancer Activities. *Chem. Biol. Drug Des.* **2021**, *97* (3), 572–591. <https://doi.org/10.1111/cbdd.13795>.
- [9]Siwach, A.; Verma, P. K. Therapeutic Potential of Oxadiazole or Furadiazole Containing Compounds. *BMC Chem.* **2020**, *14* (1), 1–40. <https://doi.org/10.1186/s13065-020-00721-2>.
- [10]El-Sayed, N. A.; Nour, M. S.; Salem, M. A.; Arafa, R. K. New Oxadiazoles with Selective-COX-2 and EGFR Dual Inhibitory Activity: Design, Synthesis, Cytotoxicity Evaluation and in Silico Studies. *Eur. J. Med. Chem.* **2019**, *183*, 111693. <https://doi.org/10.1016/j.ejmech.2019.111693>.
- [11]Polothi, R.; Raolji, G. S. B.; Kuchibhotla, V. S.; Sheelam, K.; Tuniki, B.; Thodupunuri, P. Synthesis and Biological Evaluation of 1,2,4-Oxadiazole Linked 1,3,4-Oxadiazole Derivatives as Tubulin Binding Agents. *Synth. Commun.* **2019**, *49* (13), 1603–1612. <https://doi.org/10.1080/00397911.2018.1535076>.
- [12]Liu, K.; Lu, X.; Zhang, H.-J.; Sun, J.; Zhu, H.-L. Synthesis, Molecular Modeling and Biological Evaluation of 2-(Benzylthio)-5-Aryloxadiazole Derivatives as Anti-Tumor Agents. *Eur. J. Med. Chem.* **2012**, *47*, 473–478. <https://doi.org/10.1016/j.ejmech.2011.11.015>.
- [13]Alam, M. M.; Nazreen, S.; Almalki, M. S.; Elhenawy, A. A.; Alsenani, N. I.; Elbehairi, S. E. I.; Malebari, A. M.; Alfaifi, M. Y.; Alsharif, M. A.; Alfaifi, S. Y. Naproxen Based 1, 3, 4-Oxadiazole Derivatives as EGFR Inhibitors: Design, Synthesis, Anticancer, and Computational Studies. *Pharmaceuticals* **2021**, *14* (9), 870. <https://doi.org/10.3390/ph14090870>.
- [14]Sever, B.; Altıntop, M. D.; Özdemir, A.; Akalın Çiftçi, G.; Ellakwa, D. E.; Tateishi, H.; Radwan, M. O.; Ibrahim, M. A. A.; Otsuka, M.; Fujita, M.; Ciftci, H. I.; Ali, T. F. S. In Vitro and In Silico Evaluation of Anticancer Activity of New Indole-Based 1,3,4-Oxadiazoles as EGFR and COX-2 Inhibitors. *Molecules* **2020**, *25* (21), 5190. <https://doi.org/10.3390/molecules25215190>.
- [15]Fathi, M. A. A.; Abd El-Hafeez, A. A.; Abdelhamid, D.; Abbas, S. H.; Montano, M. M.; Abdel-Aziz, M. 1,3,4-Oxadiazole/Chalcone Hybrids: Design, Synthesis, and Inhibition of Leukemia Cell Growth and EGFR, Src, IL-6 and STAT3 Activities. *Bioorganic Chem.* **2019**, *84*, 150–163. <https://doi.org/10.1016/j.bioorg.2018.11.032>.
- [16]Choudhary, S.; Arora, M.; Verma, H.; Kumar, M.; Silakari, O. Benzimidazole Based Hybrids against Complex Diseases: A Catalogue of the SAR Profile. *Eur. J. Pharmacol.* **2021**, *899*, 174027. <https://doi.org/10.1016/j.ejphar.2021.174027>.
- [17]Feng, L.-S.; Su, W.-Q.; Cheng, J.-B.; Xiao, T.; Li, H.-Z.; Chen, D.-A.; Zhang, Z.-L. Benzimidazole Hybrids as Anticancer Drugs: An Updated Review on Anticancer Properties, Structure–Activity Relationship, and Mechanisms of Action (2019–2021). *Arch. Pharm. (Weinheim)* **2022**, *355* (6), 2200051. <https://doi.org/10.1002/ardp.202200051>.

- [18]Lee, Y. T.; Tan, Y. J.; Oon, C. E. Benzimidazole and Its Derivatives as Cancer Therapeutics: The Potential Role from Traditional to Precision Medicine. *Acta Pharm. Sin. B* **2022**. <https://doi.org/10.1016/j.apsb.2022.09.010>.
- [19]Akhtar, Md. J.; Khan, A. A.; Ali, Z.; Dewangan, R. P.; Rafi, Md.; Hassan, Md. Q.; Akhtar, Md. S.; Siddiqui, A. A.; Partap, S.; Pasha, S.; Yar, M. S. Synthesis of Stable Benzimidazole Derivatives Bearing Pyrazole as Anticancer and EGFR Receptor Inhibitors. *Bioorganic Chem.* **2018**, *78*, 158–169. <https://doi.org/10.1016/j.bioorg.2018.03.002>.
- [20]Chhahed, S. S.; Sonawane, S. S.; Upasani, C. D.; Kshirsagar, S. J.; Gupta, P. P. Design, Synthesis and Molecular Modeling Studies of Few Chalcone Analogues of Benzimidazole for Epidermal Growth Factor Receptor Inhibitor in Search of Useful Anticancer Agent. *Comput. Biol. Chem.* **2016**, *61*, 138–144. <https://doi.org/10.1016/j.compbiolchem.2016.02.001>.
- [21]Gillet, J.-P.; Calcagno, A. M.; Varma, S.; Marino, M.; Green, L. J.; Vora, M. I.; Patel, C.; Orina, J. N.; Eliseeva, T. A.; Singal, V. Redefining the Relevance of Established Cancer Cell Lines to the Study of Mechanisms of Clinical Anti-Cancer Drug Resistance. *Proc. Natl. Acad. Sci.* **2011**, *108* (46), 18708–18713. DOI: 10.1073/pnas.1111840108.
- [22]Ngilirabanga, J. B.; Samsodien, H. Pharmaceutical Co-crystal: An Alternative Strategy for Enhanced Physicochemical Properties and Drug Synergy. *Nano Sel.* **2021**, *2* (3), 512–526. DOI: 10.1002/nano.202000201.
- [23]Akhtar, M. J.; Siddiqui, A. A.; Khan, A. A.; Ali, Z.; Dewangan, R. P.; Pasha, S.; Yar, M. S. Design, Synthesis, Docking and QSAR Study of Substituted Benzimidazole Linked Oxadiazole as Cytotoxic Agents, EGFR and ErbB2 Receptor Inhibitors. *Eur. J. Med. Chem.* **2017**, *126*, 853–869. <https://doi.org/10.1016/j.ejmech.2016.12.014>.
- [24]Katikireddy, R.; Marri, S.; Kakkerla, R.; Murali Krishna, M. P. S.; Gandamalla, D.; Reddy, Y. N. Synthesis, Anticancer Activity and Molecular Docking Studies of Hybrid Benzimidazole-1, 3, 4-Oxadiazole-2-N-Alkyl/Aryl Amines. *Polycycl. Aromat. Compd.* **2021**, 1–15. DOI:10.1080/10406638.2021.1959352.
- [25]Abdullah Alzahrani, H.; Mahboob Alam, M.; A. Elhenawy, A. Synthesis, Antimicrobial, Antiproliferative, and Docking Studies of 1,3,4-Oxadiazole Derivatives Containing Benzimidazole Scaffold. *19.07.2022* **2022**, *13* (3), 1–16. <https://doi.org/10.33263/BRIAC133.298>.
- [26]Jiang, Y.; Jia, S.; Li, X.; Sun, Y.; Li, W.; Zhang, W.; Xu, G. An Efficient NaHSO₃-Promoted Protocol for Chemoselective Synthesis of 2-Substituted Benzimidazoles in Water. *Chem. Pap.* **2018**, *72* (5), 1265–1276. DOI:10.1007/s11696-017-0367-5
- [27]Ahmed, F. F.; Abd El-Hafeez, A. A.; Abbas, S. H.; Abdelhamid, D.; Abdel-Aziz, M. New 1,2,4-Triazole-Chalcone Hybrids Induce Caspase-3 Dependent Apoptosis in A549 Human Lung Adenocarcinoma Cells. *Eur. J. Med. Chem.* **2018**, *151*, 705–722. <https://doi.org/10.1016/j.ejmech.2018.03.073>.
- [28]Wildman, S. A.; Crippen, G. M. Prediction of Physicochemical Parameters by Atomic Contributions. *J. Chem. Inf. Comput. Sci.* **1999**, *39* (5), 868–873. DOI: 10.1021/ci9903071.
- [29]Lovering, F.; Bikker, J.; Humblet, C. Escape from Flatland: Increasing Saturation as an Approach to Improving Clinical Success. *J. Med. Chem.* **2009**, *52* (21), 6752–6756. <https://doi.org/10.1021/jm901241e>.
- [30]Ritchie, T. J.; Ertl, P.; Lewis, R. The Graphical Representation of ADME-Related Molecule Properties for Medicinal Chemists. *Drug Discov. Today* **2011**, *16* (1–2), 65–72. DOI: 10.1016/j.drudis.2010.11.002.
- [31]Karaaslan, C.; Duydu, Y.; Ustundag, A.; Yalcin, C. O.; Kaskatepe, B.; Goker, H. Synthesis & Anticancer Evaluation of New Substituted 2-(3,4-Dimethoxyphenyl)Benzazoles. *Med. Chem.* **2019**, *15* (3), 287–297. <https://doi.org/10.2174/1573406414666180711130012>.
- [32]Jiang, Y.; Jia, S.; Li, X.; Sun, Y.; Li, W.; Zhang, W.; Xu, G. An Efficient NaHSO₃-Promoted Protocol for Chemoselective Synthesis of 2-Substituted Benzimidazoles in Water. *Chem. Pap.* **2018**, *72* (5), 1265–1276. <https://doi.org/10.1007/s11696-017-0367-5>.
- [33]Kurdekar, V.; Giridharan, S.; Subbarao, J.; Nijaguna, M. B.; Periasamy, J.; Boggaram, S.; Shivange, A. V.; Sadasivam, G.; Padigar, M.; Potluri, V.; Venkitaraman, A. R.; Bharatham, K. Structure-Guided Synthesis and Evaluation of Small-Molecule Inhibitors Targeting Protein–Protein Interactions of BRCA1 TBRCT Domain. *ChemMedChem* **2019**, *14* (18), 1620–1632. <https://doi.org/10.1002/cmdc.201900300>.
- [34]Rostamizadeh, S.; Aryan, R.; Ghaieni, H. R.; Amani, A. M. Solvent-Free Chemoselective Synthesis of Some Novel Substituted 2-Arylbenzimidazoles Using Amino Acid-Based Protonium Nitrate Ionic Liquid as Catalyst. *J. Heterocycl. Chem.* **2009**, *46* (1), 74–78. <https://doi.org/10.1002/jhet.35>.
- [35]Maiti, D. K.; Halder, S.; Pandit, P.; Chatterjee, N.; De Joarder, D.; Pramanik, N.; Saima, Y.; Patra, A.; Maiti, P. K. Synthesis of Glycal-Based Chiral Benzimidazoles by VO(AcAc)₂-CeCl₃ Combo Catalyst and Their Self-Aggregated Nanostructured Materials. *J. Org. Chem.* **2009**, *74* (21), 8086–8097. <https://doi.org/10.1021/jo901458k>.
- [36]Göker, H.; Tunçbilek, M.; Süzen, S.; Kus, C.; Altanlar, N. Synthesis and Antimicrobial Activity of Some New 2-Phenyl-N-substituted Carboxamido-1H-benzimidazole Derivatives. *Arch. Pharm. Int. J. Pharm. Med. Chem.* **2001**, *334* (5), 148–152. DOI: 10.1002/1521-4184(200105)334:5<148::aid-ardp148>3.0.co;2-s
- [37]Sri Ramya, P. V.; Angapelly, S.; Rani, R. S.; Digwal, C. S.; Ganesh Kumar, C.; Nagendra Babu, B.; Guntuku, L.; Kamal, A. Hypervalent Iodine(III) Catalyzed Rapid and Efficient Access to Benzimidazoles, Benzothiazoles and Quinoxalines: Biological Evaluation of Some New Benzimidazole-Imidazo[1,2-a]Pyridine Conjugates. *Arab. J. Chem.* **2020**, *13* (1), 120–133. <https://doi.org/10.1016/j.arabjc.2017.02.007>.
- [38]Behrouz, S. Copper-Doped Silica Cuprous Sulfate: A Highly Efficient Heterogeneous Nano-Catalyst for One-Pot Three-Component Synthesis of 1-H-2-Substituted Benzimidazoles from 2-Bromoanilines, Aldehydes, and [Bmim]N₃. *J. Saudi Chem. Soc.* **2018**, *22* (3), 261–268. <https://doi.org/10.1016/j.jscs.2016.07.003>.
- [39]Yeong, K. Y.; Chia, T. S.; Quah, C. K.; Tan, S. C. Synthesis and Crystal Structures of Ethyl 2-(4-Methoxyphenyl)-1H-Benzo[d]Imidazole-5-Carboxylate Dihydrate and Its Building Block 4-Fluoro-3-Nitrobenzoic Acid. *J. Chem. Crystallogr.* **2018**, *48* (4), 170–176. <https://doi.org/10.1007/s10870-018-0725-3>.
- [40]Azizian, H.; Pedrood, K.; Moazzam, A.; Valizadeh, Y.; Khavanizadeh, K.; Zamani, A.; Mohammadi-Khanaposhani, M.; Mojtavavi, S.; Faramarzi, M. A.; Hosseini, S.; Sarrafi, Y.; Adibi, H.; Larijani, B.; Rastegar, H.; Mahdavi, M. Docking Study, Molecular Dynamic, Synthesis, Anti- α -Glucosidase Assessment, and ADMET Prediction of New Benzimidazole-Schiff Base Derivatives. *Sci. Rep.* **2022**, *12* (1), 14870. <https://doi.org/10.1038/s41598-022-18896-0>.
- [41]O'Boyle, N. M.; Banck, M.; James, C. A.; Morley, C.; Vandermeersch, T.; Hutchison, G. R. Open Babel: An Open Chemical Toolbox. *J. Cheminformatics* **2011**, *3* (1), 33. <https://doi.org/10.1186/1758-2946-3-33>.
- [42]Morris, G. M.; Huey, R.; Lindstrom, W.; Sanner, M. F.; Belew, R. K.; Goodsell, D. S.; Olson, A. J. AutoDock4 and AutoDockTools4: Automated Docking with Selective Receptor Flexibility. *J. Comput. Chem.* **2009**, *30* (16), 2785–2791. <https://doi.org/10.1002/jcc.21256>.
- [43]Stamos, J.; Sliwkowski, M. X.; Eigenbrot, C. Structure of the Epidermal Growth Factor Receptor Kinase Domain Alone and in Complex with a 4-Anilinoquinazoline Inhibitor *. *J. Biol. Chem.* **2002**, *277* (48), 46265–46272. <https://doi.org/10.1074/jbc.M207135200>.
- [44]Eastman, P.; Friedrichs, M. S.; Chodera, J. D.; Radmer, R. J.; Bruns, C. M.; Ku, J. P.; Beauchamp, K. A.; Lane, T. J.; Wang, L.-P.; Shukla, D.; Tye, T.; Houston, M.; Stich, T.; Klein, C.; Shirts, M. R.; Pande, V. S. OpenMM 4: A Reusable, Extensible, Hardware Independent Library for High Performance Molecular Simulation. *J. Chem. Theory Comput.* **2013**, *9* (1), 461–469. <https://doi.org/10.1021/ct300857j>.
- [45]Dallakyan, S.; Olson, A. J. Small-Molecule Library Screening by Docking with PyRx. In *Chemical Biology: Methods and Protocols*; Hempel, J. E., Williams, C. H., Hong, C. C., Eds.; Methods in Molecular Biology; Springer: New York, NY, 2015; pp 243–250. https://doi.org/10.1007/978-1-4939-2269-7_19.
- [46]Seeliger, D.; de Groot, B. L. Ligand Docking and Binding Site Analysis with PyMOL and Autodock/Vina. *J. Comput. Aided Mol. Des.* **2010**, *24* (5), 417–422. <https://doi.org/10.1007/s10822-010-9352-6>.